PHILOSOPHICAL TRANSACTIONS OF THE ROYAL SOCIETY A
MATHEMATICAL, PHYSICAL & ENGINEERING SCIENCES

The Construction of Displacement Fields of Dislocation Loops and Stacking-Fault Tetrahedra from Angular Dislocation Segments

D. K. Saldin and M. J. Whelan

Phil. Trans. R. Soc. Lond. A 1979 **292**, 513-521
doi: 10.1098/rsta.1979.0071

THE CONSTRUCTION OF DISPLACEMENT FIELDS OF DISLOCATION LOOPS AND STACKING-FAULT TETRAHEDRA FROM ANGULAR DISLOCATION SEGMENTS

By D. K. SALDIN and M. J. WHELAN, F.R.S.
Department of Metallurgy and Science of Materials, University of Oxford, Parks Road, Oxford OX1 3PH, U.K.

(*Received* 16 *November* 1978)

CONTENTS

The computer simulation of electron microscope images of lattice defects requires detailed knowledge of the displacement fields of the defects. By using the method of Yoffe (1960), expressions are derived for the displacement field of a regular *N*-sided polygonal dislocation loop of arbitrary Burgers vector, and of a stacking-fault tetrahedron, in forms suitable for use in image simulation.

1. Introduction

The interpretation of electron microscope images from small dislocation loops in metals has been greatly facilitated by the use of the technique (Head 1967) for generating computer simulated images (see, for example, Maher *et al.* 1971; Bullough *et al.* 1971; Wilkens & Ruhle 1972; Hausserman *et al.* 1972). The latter two papers employ the infinitesimal loop model (Eshelby 1957; Kroupa 1963). The former two papers employ an improved model of the loop strain-field, namely that derived for a finite circular edge dislocation loop (Kroupa 1960; Bullough & Newman 1960). The work has been extended to the study of finite circular loops with shear components of Burgers vector by Holmes *et al.* (1976) who combined the strain-field of an edge dislocation loop with that of a pure shear dislocation loop derived by Ohr (1972).

In this paper we describe a more versatile method of constructing the displacement fields due to small defect clusters (on the basis of isotropic elasticity theory): they are built up from angular dislocation segments (Yoffe 1960). This technique facilitates the construction of the displacement fields of dislocation loops of various shapes (e.g. triangular, square, hexagonal and in the limit of a large number of sides, circular, with arbitrary edge and shear components), as well as those of more complicated defects such as stacking-fault tetrahedra. Also, the displacement field expressions thus calculated are analytic (unlike those previously used for the finite circular dislocation loop) and do not require prior evaluation, thus resulting in a saving of computer time.

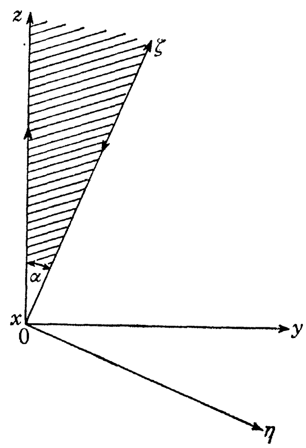

FIGURE 1. An angular dislocation.

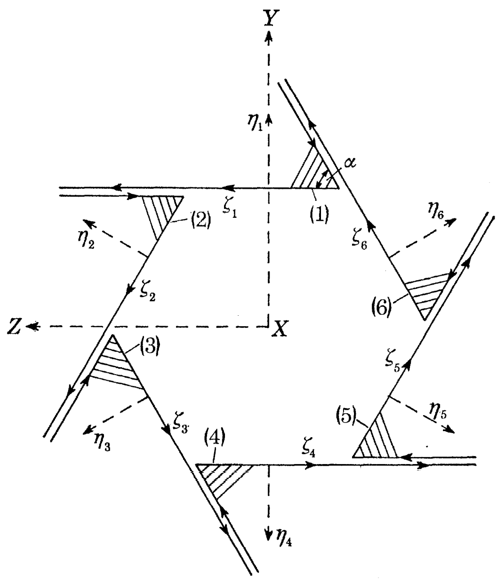

FIGURE 2. Construction of a hexagonal dislocation loop from angular dislocation segments.

2. Construction of the displacement fields

(a) *Regular polygonal dislocation loop*

Figure 1 illustrates an angular dislocation. It consists of two semi-infinite arms of dislocation line (lying along the positive z and ζ axes) enclosing a cut in the elastic continuum involving a discontinuity in the displacement field of magnitude $\boldsymbol{b}$, the Burgers vector. Let the components of $\boldsymbol{b}$ in the directions of the x, y and z axes be b_x, b_y, and b_z. Substitution of these values into the

PHILOSOPHICAL TRANSACTIONS OF THE ROYAL SOCIETY A MATHEMATICAL, PHYSICAL & ENGINEERING SCIENCES

formulae of Yoffe (1960) (see appendix) determines the components (u, v, w) in the directions of the $\boldsymbol{x}$, $\boldsymbol{y}$ and $\boldsymbol{z}$ axes of the displacement field at a general point $P(\mathrm{x}, \mathrm{y}, \mathrm{z})$ due to the angular dislocation.

Consider now figure 2, which illustrates a regular hexagonal dislocation loop, constructed from six angular dislocations. The loop as a whole is described in terms of a right-handed Cartesian system of axes $\boldsymbol{X}$, $\boldsymbol{Y}$, $\boldsymbol{Z}$, while its constituent angular dislocations are described by the right-handed Cartesian axes $\boldsymbol{X}$, $\boldsymbol{\eta}_j$, $\boldsymbol{\zeta}_j$, where j takes the values from 1 to N (N being the number of sides of the polygon). If the Burgers vectors of all the angular dislocations are equal, then the resultant effect is that due to an N-sided polygonal dislocation loop, because of the cancellation of the overlapping dislocation segments of opposite sign. Let the Burgers vector of the resultant loop have components (b_x, b_y, b_z). Then if the Burgers vector components of the angular dislocations j, with respect to the axes $\boldsymbol{X}$, $\boldsymbol{\eta}_j$, $\boldsymbol{\zeta}_j$ are given by $(b_{xj}, b_{\eta j}, b_{\zeta j})$,

$$\left.\begin{aligned} b_{xj} &= b_X \quad (\text{for all } j), \\ \text{and} \qquad \begin{pmatrix} b_{\eta j} \\ b_{\zeta j} \end{pmatrix} &= \boldsymbol{A}_j \begin{pmatrix} b_y \\ b_z \end{pmatrix}, \end{aligned}\right\} \tag{1}$$

where
$$\boldsymbol{A}_j = \begin{pmatrix} \cos\theta_j & \sin\theta_j \\ -\sin\theta_j & \cos\theta_j \end{pmatrix};$$

θ_j is the angle between $\boldsymbol{\eta}_j$ and $\boldsymbol{Y}$, measured anticlockwise from $\boldsymbol{Y}$, and thus equal to $(j-1)\,2\pi/N$.

We require to evaluate displacement field components (U, V, W) with respect to the $\boldsymbol{X}$, $\boldsymbol{Y}$, $\boldsymbol{Z}$ axes, at the general point $P(X, Y, Z)$ due to the loop. Let the coordinates of P with respect to the axes $\boldsymbol{X}$, $\boldsymbol{\eta}_j$, $\boldsymbol{\zeta}_j$ be (x_j, η_j, ζ_j). Then we have also

$$\left.\begin{aligned} x_j &= X \quad (\text{for all } j). \\ \text{and} \qquad \begin{pmatrix} \eta_j + h\cos\frac{1}{2}\alpha \\ \zeta_j \end{pmatrix} &= \boldsymbol{A}_j \begin{pmatrix} Y \\ Z \end{pmatrix}, \end{aligned}\right\} \tag{2}$$

where h is the distance from the centroid of the polygon to a vertex and $\alpha = 2\pi/N$.

Let (u_j, v_j, w_j) be the components in the directions of the axes $\boldsymbol{X}$, $\boldsymbol{\eta}_j$, $\boldsymbol{\zeta}_j$ of the displacement field contributed by the jth angular dislocation at P. These components of the displacement field can be evaluated from Yoffe's (1960) formulae by suitable substitutions of the vectors $(b_{xj}, b_{\eta j}, b_{\zeta j})$ and by identification in her formulae of the following:

$$\left.\begin{aligned} \mathrm{y} &\to \eta_j, \\ z &\to \zeta_j + h\sin\tfrac{1}{2}\alpha, \\ \eta &\to \eta_{j-1}, \\ \zeta &\to \zeta_{j-1} - h\sin\tfrac{1}{2}\alpha. \end{aligned}\right\} \tag{3}$$

Finally we have the relations

$$\left.\begin{aligned} U &= \sum_{j=1}^{N} u_j, \\ \text{and} \qquad \begin{pmatrix} V \\ W \end{pmatrix} &= \sum_{j=1}^{N} \boldsymbol{C}_j \begin{pmatrix} v_j \\ w_j \end{pmatrix}, \end{aligned}\right\} \tag{4}$$

where $\boldsymbol{C}_j = \boldsymbol{A}_j^{-1}$.

It will be observed that although the diagram in figure 2 refers to the special case a of hexagonal dislocation loop, all of the above formulae are applicable to the regular N-sided polygon (where N takes any integral value greater than 2). Thus in the limit where N becomes large, the displacement field is a good approximation to that of a circular dislocation loop. It is also

PHILOSOPHICAL TRANSACTIONS OF THE ROYAL SOCIETY A MATHEMATICAL, PHYSICAL & ENGINEERING SCIENCES

apparent from an examination of Yoffe's formulae that, by using the FS/RH convention of Bilby *et al.* (1955) for defining the sign of the Burgers vector, the method introduces a discontinuity in the displacement field vector $\boldsymbol{R}(X, Y, Z)$ of magnitude $-\boldsymbol{b}$ on crossing the region of the plane $X = 0$ which lies outside the perimeter of the loop from positive to negative X (where $\boldsymbol{b}$ is the Burgers vector of the loop). The displacement field can now be adjusted by adding a vector of magnitude $\boldsymbol{b}$ to $\boldsymbol{R}(X, Y, Z)$ for negative X, while $\boldsymbol{R}(X, Y, Z)$ for positive X is unaltered. This

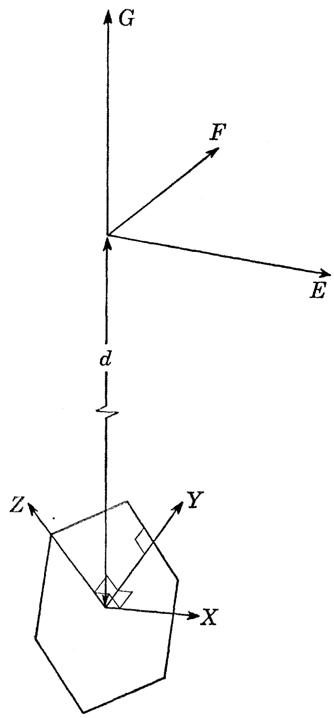

FIGURE 3. Positioning and orientation of a dislocation loop in a foil.

transfers the discontinuity in the displacement field to the inside of the loop. The magnitude of the discontinuity is now $\boldsymbol{b}$ on crossing this area from positive to negative x. This transformation does not alter the strain field (which is related to the derivatives of the displacement field in the regions where the displacement field is continuous). The equations of elasticity only strictly determine the strains, and the displacement fields so derived are arbitrary to the extent of constants of integration, and this provides the justification for the above procedure. When $\boldsymbol{b}$ is not equal to a perfect lattice vector (as for instance in the case of a Frank loop) this construction automatically introduces a stacking fault inside the loop. It is also clear from the FS/RH rule that if $\boldsymbol{b}$ is specified with a component in the direction of the positive $\boldsymbol{X}$ axis, the loop is of vacancy character and if it has a component in the opposite direction, it is of interstitial character.

Finally, in any practical application in electron microscope image calculations it is necessary to specify the depth and the orientation of the loop relative to a system of axes with origin at the electron entry surface of the foil and fixed relative to the foil. Figure 3 shows such a system consisting of right-handed Cartesian axes $\boldsymbol{E}$, $\boldsymbol{F}$, $\boldsymbol{G}$ with $\boldsymbol{G}$ antiparallel to the direction of electron

PHILOSOPHICAL TRANSACTIONS OF THE ROYAL SOCIETY A MATHEMATICAL, PHYSICAL & ENGINEERING SCIENCES

flow. The origin of the $\boldsymbol{X}$, $\boldsymbol{Y}$, $\boldsymbol{Z}$ system is placed at $(0, 0, -d)$ in the $\boldsymbol{E}$, $\boldsymbol{F}$, $\boldsymbol{G}$ system. If (e, f, g) are coordinates of P on the latter system of axes we have

$$\begin{pmatrix} X \\ Y \\ Z \end{pmatrix} = \begin{pmatrix} \hat{\boldsymbol{X}}\cdot\hat{\boldsymbol{E}} & \hat{\boldsymbol{X}}\cdot\hat{\boldsymbol{F}} & \hat{\boldsymbol{X}}\cdot\hat{\boldsymbol{G}} \\ \hat{\boldsymbol{Y}}\cdot\hat{\boldsymbol{E}} & \hat{\boldsymbol{Y}}\cdot\hat{\boldsymbol{F}} & \hat{\boldsymbol{Y}}\cdot\hat{\boldsymbol{G}} \\ \hat{\boldsymbol{Z}}\cdot\hat{\boldsymbol{E}} & \hat{\boldsymbol{Z}}\cdot\hat{\boldsymbol{F}} & \hat{\boldsymbol{Z}}\cdot\hat{\boldsymbol{G}} \end{pmatrix} \begin{pmatrix} e \\ f \\ (g+d) \end{pmatrix}, \tag{5}$$

where the symbol $\wedge$ indicates a unit vector in the direction of the corresponding axis.

Equations (4) express the displacement field $\boldsymbol{R}$ due to the loop in terms of its components (U, V, W) in the direction of the axes $(\boldsymbol{X}, \boldsymbol{Y}, \boldsymbol{Z})$. In the computation of diffraction intensities from a deformed crystal, it is necessary to know the value of the phase angle $2\pi \boldsymbol{g}\cdot\boldsymbol{R}$ as a function of position (where $\boldsymbol{g}$ is the reciprocal lattice vector of the operating Bragg reflexion). But $\boldsymbol{g}$ is usually expressed in terms of its Miller indices (h, k, l) where $\boldsymbol{g} = h\boldsymbol{a}^* + k\boldsymbol{b}^* + l\boldsymbol{c}^*$ $(\boldsymbol{a}^*, \boldsymbol{b}^*, \boldsymbol{c}^*$ are reciprocal lattice vectors). It is therefore convenient to express $\boldsymbol{R}$ in the form $\boldsymbol{R} = R_1\boldsymbol{a} + R_2\boldsymbol{b} + R_3\boldsymbol{c}$ (where $\boldsymbol{a}$, $\boldsymbol{b}$, $\boldsymbol{c}$ are the corresponding direct lattice vectors). It then follows that

$$\begin{pmatrix} R_1 \\ R_2 \\ R_3 \end{pmatrix} = \begin{pmatrix} \hat{\boldsymbol{X}}\cdot\boldsymbol{a}^* & \hat{\boldsymbol{Y}}\cdot\boldsymbol{a}^* & \hat{\boldsymbol{Z}}\cdot\boldsymbol{a}^* \\ \hat{\boldsymbol{X}}\cdot\boldsymbol{b}^* & \hat{\boldsymbol{Y}}\cdot\boldsymbol{b}^* & \hat{\boldsymbol{Z}}\cdot\boldsymbol{b}^* \\ \hat{\boldsymbol{X}}\cdot\boldsymbol{c}^* & \hat{\boldsymbol{Y}}\cdot\boldsymbol{c}^* & \hat{\boldsymbol{Z}}\cdot\boldsymbol{c}^* \end{pmatrix} \begin{pmatrix} U \\ V \\ W \end{pmatrix}. \tag{6}$$

Thus the vector displacement field (R_1, R_2, R_3) of an arbitrarily orientated dislocation loop loop at an arbitrary depth d from the electron-entry surface may be found.

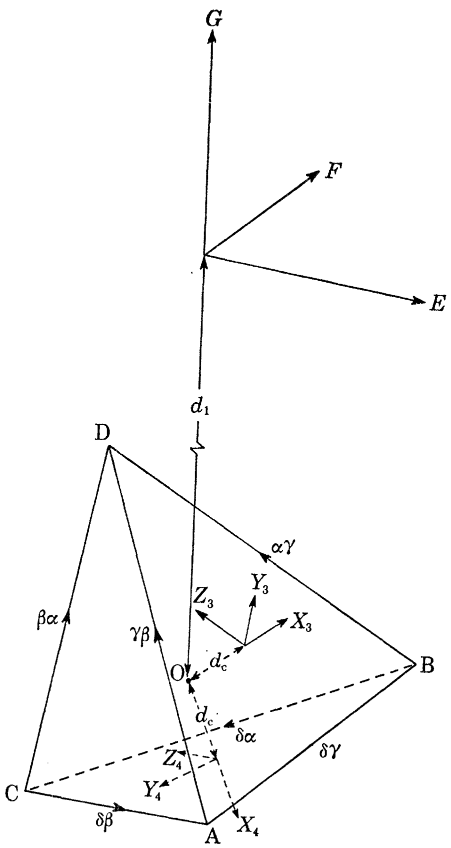

FIGURE 4. A stacking-fault tetrahedron and its positioning and orientation in a foil.

(*b*) *The stacking-fault tetrahedron*

A diagram of a stacking-fault tetrahedron is shown in figure 4. Each of the six edges consists of a stair-rod dislocation whose Burgers vector is shown in Thomson's (1953) notation. Consider the faces a, b, c and d to be composed of triangular edge dislocation loops of Burgers vectors **Oα**, **Oβ**, **Oγ** and **Oδ** respectively (**O** is the centroid of the Thompson tetrahedron). At the lines of contact of their edges, e.g. CD, the resultant Burgers vector is obtained by merely adding those of the loops in contact. For example, the Burgers vector of the dislocation CD is given by:

$$\boldsymbol{\beta}\mathbf{O} + \mathbf{O}\boldsymbol{\alpha} \rightarrow \boldsymbol{\beta}\boldsymbol{\alpha},$$

which is precisely the Burgers vector of the stair-rod dislocation on the corresponding edge of the stacking-fault tetrahedron. This is essentially the technique employed to construct the displacement field of the stacking-fault tetrahedron. Triangular edge dislocation loops are constructed by methods described in (*a*) and are positioned so as to form a tetrahedron.

Let the right-handed coordinate systems (analogous to the $\boldsymbol{X}$, $\boldsymbol{Y}$, $\boldsymbol{Z}$ system in (*a*)) on each of the triangular faces be $\boldsymbol{X}_\mu$, $\boldsymbol{Y}_\mu$, $\boldsymbol{Z}_\mu$, where μ takes the values 1–4. We consider a tetrahedron whose centroid lies at a depth d_1 below the electron entry surface. It is useful to describe this in terms of the $\boldsymbol{E}$, $\boldsymbol{F}$, $\boldsymbol{G}$ system considered in (*a*). Let the centroid of the tetrahedron be at the point $(0, 0, -d_1)$ in the $\boldsymbol{E}$, $\boldsymbol{F}$, $\boldsymbol{G}$ system, and let the distance from the centroid to any of the faces of the tetrahedron be d_c. If the coordinates of the general point P in the $\boldsymbol{E}$, $\boldsymbol{F}$, $\boldsymbol{G}$ system are (e, f, g), then its coordinates with respect to the axes $\boldsymbol{X}_\mu$, $\boldsymbol{Y}_\mu$, $\boldsymbol{Z}_\mu$, namely (X_μ, Y_μ, Z_μ) are determined by the equations

$$\begin{pmatrix} (X_\mu + d_c) \\ Y_\mu \\ Z_\mu \end{pmatrix} = \begin{pmatrix} \hat{\boldsymbol{E}}\cdot\hat{\boldsymbol{X}}_\mu & \hat{\boldsymbol{F}}\cdot\hat{\boldsymbol{X}}_\mu & \hat{\boldsymbol{G}}\cdot\hat{\boldsymbol{X}}_\mu \\ \hat{\boldsymbol{E}}\cdot\hat{\boldsymbol{Y}}_\mu & \hat{\boldsymbol{F}}\cdot\hat{\boldsymbol{Y}}_\mu & \hat{\boldsymbol{G}}\cdot\hat{\boldsymbol{Y}}_\mu \\ \hat{\boldsymbol{E}}\cdot\hat{\boldsymbol{Z}}_\mu & \hat{\boldsymbol{F}}\cdot\hat{\boldsymbol{Z}}_\mu & \hat{\boldsymbol{G}}\cdot\hat{\boldsymbol{Z}}_\mu \end{pmatrix} \begin{pmatrix} e \\ f \\ (g + d_1) \end{pmatrix}. \tag{7}$$

If l is the length of each edge of the tetrahedron,

$$d_c = \tfrac{1}{4}\sqrt{\tfrac{2}{3}}\, l$$

Let $\mu = 1, 2, 3$ and 4 correspond to the faces a, b, c and d respectively of the Thompson tetrahedron. The tetrahedron may be orientated by specifying the axes $\boldsymbol{X}_4$, $\boldsymbol{Y}_4$, $\boldsymbol{Z}_4$. These are [111], [$2\bar{1}\bar{1}$] and [$01\bar{1}$] respectively. The axes for $\mu = 1, 2$ and 3 may be generated from $\hat{\boldsymbol{X}}_4$, $\hat{\boldsymbol{Y}}_4$, $\hat{\boldsymbol{Z}}_4$ by rotations of 180° about the axes [100], [010] and [001] respectively, and we thus have,

$$\left.\begin{aligned} \hat{\boldsymbol{X}}_\mu &= \boldsymbol{M}_\mu \hat{\boldsymbol{X}}_4, \\ \hat{\boldsymbol{Y}}_\mu &= \boldsymbol{M}_\mu \hat{\boldsymbol{Y}}_4, \\ \hat{\boldsymbol{Z}}_\mu &= \boldsymbol{M}_\mu \hat{\boldsymbol{Z}}_4, \end{aligned}\right\} \text{ for } \quad \mu = 1,\ 2, \text{ and } 3, \tag{8}$$

where
$$\boldsymbol{M}_1 = \begin{pmatrix} 1 & 0 & 0 \\ 0 & -1 & 0 \\ 0 & 0 & -1 \end{pmatrix}, \quad \boldsymbol{M}_2 = \begin{pmatrix} -1 & 0 & 0 \\ 0 & 1 & 0 \\ 0 & 0 & -1 \end{pmatrix}, \quad \boldsymbol{M}_3 = \begin{pmatrix} -1 & 0 & 0 \\ 0 & -1 & 0 \\ 0 & 0 & 1 \end{pmatrix}.$$

Substitutions of the coordinates (x_μ, y_μ, z_μ) and the appropriate Burgers vectors into the formulae described in (*a*) determines the contributions to the displacement field from each constituent triangular loop, and appropriate additions of these expressions determine the strain-field of the stacking-fault tetrahedron.

The discontinuities in the displacement field on crossing any of the faces do not yet correspond to the stacking faults on these faces (on the face d, for example, the stacking-fault vector is of magnitude $|\mathbf{D\delta}|$). The discontinuity in the vector $\boldsymbol{R}(e, f, g)$ introduced by this technique of construction is $|\mathbf{O\delta}|$. To overcome this problem consider the addition of a displacement of magnitude **DO** to all the material inside the tetrahedron. The displacement discontinuity on face d then becomes (we are considering the case of a vacancy-type tetrahedron whose faces are traversed from positive to negative x_μ),

$$\mathbf{DO}+\mathbf{O\delta}\rightarrow\mathbf{D\delta}$$

The discontinuities on the other faces become

$$\mathbf{DO}+\mathbf{O\alpha}\rightarrow\mathbf{D\alpha}=\mathbf{DA}+\mathbf{A\alpha},$$

$$\mathbf{DO}+\mathbf{O\beta}\rightarrow\mathbf{D\beta}=\mathbf{DB}+\mathbf{B\beta},$$

$$\mathbf{DO}+\mathbf{O\gamma}\rightarrow\mathbf{D\gamma}=\mathbf{DC}+\mathbf{C\gamma}.$$

The vectors **DA**, **DB** and **DC** of course correspond to perfect lattice vectors in the *f.c.c.* lattice and thus the discontinuities on the faces a, b, and c, are **Aα**, **Bβ** and **Cγ** respectively, which are precisely the fault vectors on the corresponding faces of the stacking-fault tetrahedron, demonstrating the symmetry of the tetrahedron with respect to each of the faces. This procedure may therefore be used to construct not only the strain field but also the correct stacking faults on the faces of the tetrahedron. The displacement field of the interstitial-type tetrahedron may also be constructed by this method if the directions of the Burgers vectors of all constituent loops are reversed. This also has the effect of creating extrinsic (rather than intrinsic as for the the vacancy-type tetrahedron) stacking faults on the faces. It is interesting to note that an atom at the centroid of a stacking-fault tetrahedron occupies an interstitial site in the (hypothetical) perfect reference lattice (i.e. one corresponding to atom positions at great distance from the tetrahedron, but extrapolated to the region inside the tetrahedron).

3. Conclusions

This paper describes a versatile method of constructing the displacement field of a polygonal dislocation loop and of a stacking-fault tetrahedron from angular dislocation segments. When used with a computer program for calculating electron diffraction image contrast and an image display system, realistic computer simulated images can be obtained. Results obtained by use of this technique for identifying small defect clusters observed in thin foils after ion irradiation are presented in the accompanying paper.

The authors wish to thank Professor Sir Peter Hirsch, F.R.S., for the provision of laboratory facilities and for many useful discussions. One of us (D.K.S.) acknowledges financial support from the Atomic Energy Research Establishment, Harwell and from the Central Electricity Electricity Generating Board.

Appendix

With reference to figure 1, the displacement field components u_x, v_x, w_x due to the x-component b_x of the Burgers vector of the angular dislocation at the point P (x, y, z) or (x, η, ζ) are

$$\left.\begin{aligned} u_x &= b_x\phi + \frac{b_x}{8\pi(1-\sigma)}\left(\frac{xy}{r(r-z)} - \frac{x\eta}{r(r-\zeta)}\right), \\ v_x &= \frac{b_x}{8\pi(1-\sigma)}\left(\frac{\eta\sin\alpha}{r-\zeta} - \frac{y\eta}{r(r-\zeta)} + \frac{y^2}{r(r-z)} + (1-2\sigma)\left(\cos\alpha\ln(r-\zeta) - \ln(r-z)\right)\right), \\ w_x &= \frac{b_x}{8\pi(1-\sigma)}\left(\frac{\eta\cos\alpha}{r-\zeta} - \frac{y}{r} - \frac{\eta z}{r(r-\zeta)} - (1-2\sigma)\sin\alpha\ln(r-\zeta)\right), \end{aligned}\right\} \quad (1)$$

where σ is Poisson's ratio and ϕ is the solid angle subtended at P by the shaded area and can be written,

$$\phi = \frac{1}{4\pi}\left[\arctan\left(\frac{y}{x}\right) - \arctan\left(\frac{\eta}{x}\right) + \arctan\left(\frac{xr\sin\alpha}{x^2\cos\alpha + y\eta}\right)\right].$$

The sign in front of $(1-2\sigma)$ in the expression for w_x differs from that quoted in Yoffe's (1960) paper. The sign quoted here is the correct one. This was also pointed out by Hokanson (1963).

If u_y, v_y, w_y, are the displacement field components due to the y- component b_y of Burgers vector, then

$$\left.\begin{aligned} u_y &= \frac{b_y}{8\pi(1-\sigma)}\left(\frac{x^2\cos\alpha}{r(r-\zeta)} - \frac{x^2}{r(r-z)} - (1-2\sigma)\left(\cos\alpha\ln(r-\zeta) - \ln(r-z)\right)\right), \\ v_y &= b_y\phi + \frac{b_y x}{8\pi(1-\sigma)}\left(\frac{y\cos\alpha}{r(r-\zeta)} - \frac{\sin\alpha\cos\alpha}{r-\zeta} - \frac{y}{r(r-z)}\right), \\ w_y &= \frac{b_y x}{8\pi(1-\sigma)}\left(\frac{z\cos\alpha}{r(r-\zeta)} - \frac{\cos^2\alpha}{r-\zeta} + \frac{1}{r}\right). \end{aligned}\right\} \quad (2)$$

If u_z, v_z, w_z are the displacement field components due to the z-component b_z of Burgers vector then,

$$\left.\begin{aligned} u_z &= \frac{b_z\sin\alpha}{8\pi(1-\sigma)}\left((1-2\sigma)\ln(r-\zeta) - \frac{x^2}{r(r-\zeta)}\right), \\ v_z &= \frac{b_z x\sin\alpha}{8\pi(1-\sigma)}\left(\frac{\sin\alpha}{r-\zeta} - \frac{y}{r(r-\zeta)}\right), \\ w_z &= b_z\phi + \frac{b_z x\sin\alpha}{8\pi(1-\sigma)}\left(\frac{\cos\alpha}{r-\zeta} - \frac{z}{r(r-\zeta)}\right). \end{aligned}\right\} \quad (3)$$

The complete displacement field at P due to an angular dislocation with an arbitrary Burgers vector is found by adding the corresponding components of equations (1), (2) and (3).

References

Bilby, B. A., Bullough, R. & Smith, E. 1955 *Proc. R. Soc. Lond.* A **231**, 263.
Bullough, R., Maher, D. M. & Perrin, R. C. 1971 *Phys. Stat. Sol.* B **43**, 689.
Bullough, R. & Newman, R. C. 1960 *Phil. Mag.* **5**, 921.
Eshelby, J. D. 1957 *Proc. R. Soc. Lond.* A **241**, 376.
Hausserman, F., Ruhle, M. & Wilkens, M. 1972 *Phys. Stat. Sol.* B **50**, 445.
Head, A. K. 1967 *Aust. J. Phys.* **20**, 557.
Hokanson, J. L. 1963 *J. appl. Phys.* **34**, 2337.

MATHEMATICAL, PHYSICAL & ENGINEERING SCIENCES
THE ROYAL SOCIETY
PHILOSOPHICAL TRANSACTIONS OF

Holmes, S. M., Eyre, B. L. & Perrin, R. C. 1976 *Electron Microscopy* 1976 (ed. Brandon, D. G.). *Proc. 6th Eur. Reg. Cong.*, Jerusalem, vol. I, p. 279. Jerusalem: TAL International.
Kroupa, F. 1960 *Czech. J. Phys.* B **10**, 284.
Kroupa, F. 1963 *Czech J. Phys.* A **13**, 301.
Maher, D. M., Perrin, R. C. & Bullough, R. 1971 *Phys. Stat. Sol.* B **43**, 707.
Ohr, S. M. 1972 *Phil. Mag.* **26**, 1307.
Thompson, N. 1953 *Proc. phys. Soc.* B **66**, 481.
Wilkens, M. & Ruhle, M. 1972 *Phys. Stat. Sol.* B **49**, 749.
Yoffe, E. H. 1960 *Phil. Mag.* **5**, 161.

PHILOSOPHICAL TRANSACTIONS OF THE ROYAL SOCIETY A MATHEMATICAL, PHYSICAL & ENGINEERING SCIENCES